RESEARCH PAPER

Sustainable Valorization of Rice Straw into Functional Cellulose Hydrogels for Diclofenac Drug Delivery Applications

Suganya C[1*], Karikalan R[2], Maroniga S[1], Mahalakshmi S[1], Loganathan S[1], Jamitha V[1]

[1] Department of Pharmaceutical Technology, Mahendra Engineering College, Namakkal

[2] Department of Mechatronics Engineering, Mahendra Engineering College, Namakkal

[1*] Corresponding Author Email: suganchan2228@gmail.com

Received: 2nd Mar, 2026 | **Revised:** 14th Mar, 2026 | **Accepted:** 4th Apr, 2026 | **Available Online:** 20th Apr, 2026

ABSTRACT

Hydrogels are three-dimensional polymeric networks capable of absorbing large amounts of water while maintaining structural stability, making them attractive materials for controlled drug delivery applications. In this study, a cellulose-based hydrogel was developed and evaluated as a potential carrier for diclofenac sodium delivery. The hydrogel was prepared through a chemical crosslinking process using suitable polymeric components to form a stable network structure. The prepared hydrogels were characterized using various physicochemical and structural analysis techniques. Swelling studies demonstrated significant water absorption under different pH conditions, confirming the hydrophilic nature of the hydrogel matrix. Porosity analysis revealed values ranging from 62–75%, indicating the presence of interconnected pores that can facilitate fluid uptake and drug diffusion. Structural characterization using Fourier Transform Infrared Spectroscopy (FTIR), Scanning Electron Microscopy (SEM), and Wide-Angle X-ray Diffraction (WAXRD) confirmed polymer–drug interactions, porous morphology, and the semi-crystalline structure of the hydrogel network. Mechanical analysis showed elastic modulus values between 0.42 and 0.71 MPa, indicating suitable flexibility and mechanical stability of the hydrogel films. In-vitro drug release studies demonstrated a sustained release profile, with approximately 88.4% of diclofenac released within 180 minutes, suggesting diffusion-controlled drug release from the hydrogel matrix. Cytotoxicity evaluation using the brine shrimp lethality assay showed low mortality (12.6 ± 1.4%), indicating minimal cytotoxic effects. The developed hydrogel exhibited desirable physicochemical properties and controlled drug release behaviour, highlighting its potential as a promising platform for controlled drug delivery applications.

Keywords: Hydrogel, Cellulose, Diclofenac sodium, Controlled drug delivery, Porosity, Biomaterials.

How to cite this article: Suganya C, Karikalan R, Maroniga S, Mahalakshmi S, Loganathan S, Jamitha V. Sustainable Valorization of Rice Straw into Functional Cellulose Hydrogels for Diclofenac Drug Delivery Applications. Int J Drug Deliv Technol. 2026;16(35s):473-482. DOI: 10.25258/ijddt.16.35s.54

Source of support: Nil.

Conflict of interest: The authors declare no conflict of interest.

1.INTRODUCTION

Biopolymer-based materials have gained considerable attention in recent years due to their biodegradability, biocompatibility, and potential applications in biomedical and pharmaceutical fields [**1,2**]**.** Among these materials, hydrogels represent an important class of polymeric systems characterized by their ability to absorb and retain large amounts of water while maintaining a stable three-dimensional network structure. Hydrogels consist of crosslinked hydrophilic polymers that can swell in aqueous environments without dissolving [**3**]. Owing to their soft structure, high porosity, and tuneable mechanical properties, hydrogels have been widely investigated for biomedical applications, particularly in controlled drug delivery systems. Their porous network allows therapeutic agents to be incorporated within the matrix and released gradually over time, enabling sustained drug delivery and improved therapeutic efficiency [**2**].

Cellulose is the most abundant natural polymer found in plant biomass and has attracted significant interest as a raw material for hydrogel development. It consists of β-(1→4)-linked glucose units forming a linear polysaccharide structure that provides excellent mechanical strength, chemical stability, and biocompatibility [**4**]. Cellulose-based hydrogels combine the advantages of natural polymers with the structural features of hydrogel systems, including high water absorption capacity and interconnected porous structures. These characteristics make cellulose a promising candidate for designing sustainable biomaterials suitable for pharmaceutical and biomedical applications [**5**].

In recent years, increasing attention has been directed toward utilizing agricultural residues as renewable sources for biomaterial production. Rice straw is one of the most abundant agricultural wastes generated during rice cultivation, particularly in Asian countries. Despite its high cellulose content, rice straw is often discarded through open-field burning, which contributes to environmental pollution and greenhouse gas emissions [**6,7**]. Converting rice straw into value-added materials such as cellulose-based hydrogels

provides a sustainable strategy for agricultural waste utilization while reducing environmental impact [**8**].

Hydrogel systems can also serve as effective carriers for therapeutic agents. Diclofenac sodium, a commonly used non-steroidal anti-inflammatory drug (NSAID), is widely prescribed for the treatment of pain and inflammation. However, conventional administration routes may lead to gastrointestinal irritation and systemic side effects [**9**]. Incorporating diclofenac sodium into hydrogel matrices can provide localized and controlled drug release, thereby improving drug delivery efficiency and reducing adverse effects [**10**].

The present study aims to develop a cellulose-based hydrogel derived from rice straw and evaluate its potential as a carrier for controlled diclofenac sodium delivery. The extracted cellulose was used to prepare a hydrogel network in combination with polyvinyl alcohol, followed by drug loading and physicochemical characterization. The prepared hydrogels were further evaluated through swelling studies, porosity analysis, structural characterization techniques, and in-vitro drug release and cytotoxicity studies to assess their suitability for controlled drug delivery applications.

2. MATERIALS AND METHODS

2.1 Materials

Rice straw was collected from local fields for cellulose extraction. PVA and glutaraldehyde were used for hydrogel preparation. H_2SO_4 and NaOH were used for extraction, while NaOCl and H_2O_2 were used for bleaching. Diclofenac sodium was used as the model drug. Ethanol and distilled water served as solvents. All chemicals were of analytical grade.

2.2. Sample preparation

The collected rice straw was washed thoroughly with distilled water to remove dust and impurities and then air-dried at room temperature. The dried biomass was further shade-dried until constant weight was achieved. The dried material was ground into fine powder using a laboratory grinder and stored in airtight containers for further experimental use.

2.3. Extraction of cellulose from rice straw

The Rice straw was subjected to treatment, and cellulose extraction was carried out using the microwave-assisted extraction method at 540 W over 180 seconds in a mixture of 2 M sulfuric acid in a 1:25 ratio [**11,12**]. The precipitated part of the sample was collected by the filtration process. The gathered part was cleaned until the solution the removed of acid. The cellulose was dried in an oven. The yield was assessed using Equation, and the weight of cellulose produced was estimated.

$$Yield\ \%\ of\ cellulose = \frac{W_{final}}{W_{initial}} \times 100 \qquad (1)$$

Where W_{final} - weight of the dried cellulose, $W_{initial}$- the initial weight of the peanut shell sample.

2.4. Response surface methodology (RSM)

RSM was applied to optimize extraction conditions using H_2SO_4 as the extracting acid. Based on single-factor studies, microwave power (450–630 W), extraction time (150–210 s), and acid concentration (1–3%) were selected as key variables. A three-factor, three-level Box–Behnken design (17 runs) was used [**13**] to evaluate their effects on extraction yield (Y). The relationship between variables and response was described by a second-order polynomial equation:

$$Y - \beta_0 + \sum_{i=1}^{i}(\beta_i x_i) + \sum_{ij=1}^{ij}(\beta_{ij} X_i X_j) + \sum_{i=1}^{i}(\beta_{ii} X^2) \qquad (1)$$

Where,

Response Rice straw extraction yield, : constant, : coefficients and : factor.

2.5. Optimization Using OVAT

One-variable-at-a-time (OVAT) was used to evaluate the effect of process parameters by varying one factor while keeping others constant. Microwave power (360–720 W), irradiation time (150–270 s), and liquid-to-solid ratio (20–60 mL/g) were studied sequentially. Microwave heating enhances extraction through ionic conduction and dipole rotation, leading to rapid heating, cell wall disruption, and improved release of bioactive compounds [**14**]. Higher microwave power reduces extraction time, while lower power requires longer exposure to achieve comparable efficiency.

2.6. PH and solubility

A pH meter was used to determine the cellulose solution's pH by adding 40 ml of distilled water to a 150 ml beaker containing a 5g of sample. After five minutes of stirring, it was centrifuged, and the pH of the supernatant was determined. With 0.2 g of cellulose powder present, a beaker filled with 20 ml of 1% acetic acid solution was shaken vigorously at 250 rpm at 25 °C using a magnetic stirrer. After stirring the mixture for half an hour, the solution was filtered. Using deionised water, the insoluble portion was cleaned. Equation 3 was utilized to calculate the percentage solubility of cellulose.

$$Solubility\ \% = 100 - \frac{Weight\ of\ insoluble\ fraction}{Initial\ weight\ of\ sample} \times 100 \qquad (2)$$

2.7. Bulk density, tapped density

The bulk density was measured by putting approximately 100 mg of cellulose powder in a standard 10 mL measuring cylinder without stirring it. In the case of tapped density, 1 g of cellulose powder was transferred to a 10 mL standard measuring cylinder and the mixture was tapped softly 2 minutes. The percentage of tapped to bulk density is a measure of flowability, also known as Hausner ratio, as expressed in Equation (4) Carr's index is the assessment of compressibility and is measured via the following equation (5).

$$Hasneur\ ratio = \frac{Tapped\ density\left(\frac{mg}{m3}\right)}{Bulk\ density\left(\frac{mg}{m3}\right)} \qquad (3)$$

$$Carr's\ index\ \% = \frac{Tapped\ density\left(\frac{mg}{m3}\right) - bulk\ density\left(\frac{mg}{m3}\right)}{Tapped\ density\ \left(\frac{mg}{m3}\right)} \times 100 \quad (4)$$

2.8. Bleaching treatment using hydrogen peroxide

The bleaching treatment with NaOCl was performed according to the methodology, with modifications [**15**]. Briefly, the RS extraction residues obtained after microwave-assisted acid and alkaline pretreatments and the bleaching solution, consisting of 5 % sodium hypochlorite (NaOCl), were mixed in a ratio of 0.57 g Rice straw, were make up to 30 mL and the treatment was carried out using a microwave oven at 540 W for 210 s. At the end of the bleaching condition, the samples were filtered and washed with distilled water to remove the bleaching solution. The obtained fibres were dried in hot Air Oven and weighed. The ground fibres were analysed as to their whiteness index (WI) (Eq. (1)) through measured CIEL*a*b* colour coordinates using a colour analysis. On the basis of the bleaching optimum conditions (lowest yield and highest WI), four bleaching cycles were applied to the cellulosic fractions (Freitas et al., 2024).

$$WI = 100 - \sqrt{(100 - L*)2 + a*2 + b*2}$$

2.9. Preparation of cellulose-PVA hydrogel

Polyvinyl alcohol (PVA, 1 g) was dissolved in 10 mL of distilled water at 95 °C under constant stirring to obtain a clear solution. Cellulose (250 mg) was separately dispersed in 10 mL of distilled water and then added to the PVA solution under continuous stirring to obtain a homogeneous mixture. Two drops of concentrated sulfuric acid were added as a catalyst, followed by the addition of glutaraldehyde (1.4 mL) as the crosslinking agent. The mixture was stirred thoroughly to allow crosslinking between PVA and cellulose chains. The resulting hydrogel solution was cast onto a clean Petri dish and dried at 50 °C for 60–70 minutes to obtain uniform hydrogel films.

2.10. Drug loading

Diclofenac sodium was used as the model drug for loading into the prepared hydrogel. Initially, 50 mg of diclofenac sodium was dissolved in a small quantity of ethanol and then diluted with phosphate buffer solution (pH 7.4) to obtain a uniform drug solution. The previously prepared and dried hydrogel films were cut into small uniform pieces and immersed in the drug solution. The samples were kept at room temperature with gentle stirring for 24 hours to allow the drug molecules to diffuse into the hydrogel matrix through the swelling process. After completion of the loading process, the hydrogels were removed from the drug solution and gently rinsed with distilled water to eliminate any drug present on the surface. The drug-loaded hydrogels were then dried in a hot air oven at 40 °C and stored in a desiccator to prevent moisture absorption until further characterization studies were carried out.

3. CHARACTERIZATION

3.1. Swelling study

The swelling behaviour of the drug-loaded hydrogel was studied to evaluate its water absorption capacity under different pH conditions. Dried hydrogel discs weighing approximately 0.5 g were immersed separately in excess distilled water and buffer solutions of pH 1.2, 5.5, and 7.4 at room temperature (25 °C). At predetermined time intervals, the swollen hydrogel samples were removed from the solutions and gently blotted with filter paper to remove excess surface liquid (Zhang et al., 2020). The samples were then weighed using a digital balance. The swelling percentage of the hydrogel was calculated using the following equation:

$$Swelling(\ \%\ ) = \frac{M_t - M_0}{M_0} \times 100 \quad (6)$$

Where:

M_0 = Initial weight of hydrogel sample

M_t = Weight of hydrogel after ethanol immersion

3.2. Porosity determination

The porosity of diclofenac sodium-loaded hydrogel films was determined using the solvent displacement method [**16**]. Dried samples were cut into uniform pieces, their volume measured, and initial weight recorded (M_1). The samples were immersed in absolute ethanol for 24 hours, then removed, surface-dried, and reweighed (M_2). The percentage porosity of the hydrogel samples was calculated using the following equation:

$$Porosity\ (\%) = \frac{M_1 - M_2}{\rho V} \times 100 \quad (7)$$

Where:

M_1 = Initial weight of hydrogel sample

M_2 = Weight of hydrogel after ethanol immersion

V = Volume of hydrogel sample

ρ = Density of ethanol

3.3. Elasticity study

The mechanical elasticity of diclofenac sodium-loaded hydrogel films was evaluated using a CRE-type tensile testing machine (SATRA 566,) with a 5 kN load cell. Samples were cut into rectangular strips (50 × 15 × 0.2 mm) and stretched at a cross-head speed of 30 mm/min. Stress–strain behaviour was recorded to determine elasticity. All measurements were performed in triplicate, and average values were reported.

3.4. Hydrophilicity study

Surface hydrophilicity of diclofenac sodium-loaded hydrogel films was evaluated using contact angle measurements. Samples were mounted on glass slides, and a droplet of distilled water was placed on the surface using a micro syringe. The contact angle was measured using a goniometer (Kernco Instrument Co.,). Measurements were taken at multiple points, and average values were reported.

3.5. Fourier transform infrared spectroscopy (FTIR) analysis

The chemical structure and functional groups present in the prepared hydrogel were analysed using Fourier Transform Infrared Spectroscopy (FTIR). This analysis was carried out to identify possible interactions between the polymer matrix and diclofenac sodium (Oliveira et al., 2014). FTIR spectra of the pure drug, blank hydrogel, and drug-loaded hydrogel samples were recorded using an IR Prestige-21 FTIR spectrophotometer (Shimadzu, Japan). Each sample was scanned 200 times in order to obtain spectra with a high signal-to-noise ratio. The spectra were recorded in the wavenumber range of 4000–400 cm^{-1} with a resolution of 4 cm^{-1}. Measurements were carried out in transmittance mode using an Attenuated Total Reflectance (ATR) accessory equipped with a zinc selenide crystal.

3.6. Scanning electron microscopy (SEM) analysis

The surface morphology of the prepared diclofenac sodium loaded hydrogel films was examined using Field Emission Scanning Electron Microscopy (FE-SEM). The analysis was performed using a TESCAN MAIA3 scanning electron microscope equipped with an EDAX detector. Before imaging, [**17**] the hydrogel samples were properly prepared to obtain clear surface micrographs. Small pieces of dried hydrogel films were mounted on aluminium stubs using conductive adhesive tape. To enhance the conductivity and improve image quality, the samples were sputter coated with a thin layer of gold for approximately 120 seconds (Martin et al., 2002). This coating helps to prevent surface charging during electron beam exposure. The coated samples were then placed inside the SEM chamber and the micrographs were recorded at different magnifications to observe the surface characteristics of the hydrogel.

3.7. Wide angle x-ray diffraction (WAXRD) analysis

The crystalline characteristics of the prepared diclofenac sodium loaded hydrogel were investigated using Wide Angle X-ray Diffraction (WAXRD) analysis. This technique was used to study the structural properties and to determine the presence of crystalline or amorphous phases within the hydrogel matrix (Kumar & Koh, 2012). The diffraction patterns of the samples were recorded using a Siemens D500 X-ray diffractometer equipped with a cobalt radiation source. The measurements were carried out using Fe-filtered Co-Kα radiation. The diffraction data were collected over a 2θ range of 20° to 100° at a scan rate of 0.02° per second. During the analysis, the operating voltage and current of the instrument were maintained at 40 kV and 40 mA, respectively.

3.8. Drug entrapment efficiency (DEE)

The efficiency of drug entrapment within the prepared hydrogel was evaluated to determine the amount of drug successfully incorporated into the polymeric network (Bhatt et al., 2014). A pre-weighed quantity of diclofenac sodium loaded hydrogel was placed in phosphate buffer saline (PBS) solution of pH 7.4 and allowed to remain for 24 hours to facilitate complete extraction of the entrapped drug. After the incubation period, the solution was stirred for 15 minutes to ensure uniform distribution of the released drug and then filtered to remove hydrogel residues. The concentration of diclofenac sodium present in the filtrate was measured using a UV–Visible spectrophotometer at an absorption wavelength of 276 nm. The percentage of drug encapsulation efficiency was calculated using the following equation:

$$\text{DEE (\%)} = \frac{Actual\ drug\ content}{Theoretical\ drug\ content} \times 100 \qquad (8)$$

3.9. In-vitro drug release study

The drug release behaviour of the diclofenac sodium loaded hydrogel was investigated using a phosphate buffer saline (PBS) solution of pH 7.4 as the dissolution medium. The prepared drug loaded hydrogel film was placed in a beaker containing 100 mL of PBS solution maintained at 37 °C to simulate physiological conditions. At regular intervals of 10 minutes, 5 mL of the release medium was withdrawn from the beaker for analysis. After each sampling, an equal volume of fresh PBS solution was added in order to maintain a constant volume of the dissolution medium. The collected samples were analysed using a UV–Visible spectrophotometer at a wavelength of 276 nm to determine the concentration of diclofenac sodium released from the hydrogel matrix. The cumulative percentage of drug release was calculated and plotted against time to evaluate the drug release profile.

3.10. Drug release kinetics

The kinetics of diclofenac sodium release from the prepared hydrogel was evaluated using a USP dissolution apparatus (paddle method). The experiment was performed at a rotation speed of 50 rpm using 900 mL of dissolution medium maintained at 37 ± 0.5 °C to mimic physiological conditions. To simulate the gastrointestinal environment, a pH change dissolution method was adopted. Initially, the drug loaded hydrogel sample was placed in 0.1 N hydrochloric acid solution (pH 1.2) for the first 2 hours. After this period, tribasic sodium phosphate solution was added to the dissolution medium and the pH was adjusted to 6.8 using NaOH or HCl solution. At predetermined time intervals, 5 mL of the dissolution medium was withdrawn and replaced with an equal volume of fresh medium in order to maintain constant volume. The collected samples were filtered and analysed using a UV–Visible spectrophotometer at 276 nm to determine the amount of diclofenac sodium released from the hydrogel system. To understand the mechanism of drug release, the release data were fitted into different kinetic models such as zero-order and first-order kinetics. The zero-order kinetic model represents a constant drug release rate independent of drug concentration and is expressed as:

$$Q_t = Q_0 + K_0 t \qquad (9)$$

Where

Q_t = amount of drug released at time t
Q_0 = initial amount of drug in the hydrogel
K_0= zero-order release constant
The first-order kinetic model describes drug release that depends on the remaining drug concentration within the hydrogel matrix and is represented as:

$$\log(Q_0 - Q_t) = \log \quad Q_0 - \frac{K_t}{2.303} \qquad (10)$$

where
Q_t = amount of drug released at time t
Q_0 = initial drug concentration
K = first-order release constant.

3.11. In-vitro cytotoxicity analysis

The cytotoxicity of the prepared diclofenac sodium loaded hydrogel was evaluated using the brine shrimp lethality bioassay, which is a simple method to assess the biocompatibility of materials [**18**]. Artificial seawater was prepared and placed in a container under continuous aeration to hatch brine shrimp eggs. After approximately 24 hours, the hatched nauplii were collected from the illuminated region of the container. The assay was performed using a microtiter plate, where each well contained 0.2 mL of artificial seawater. A specific number of active nauplii were transferred into each well. The hydrogel samples were then introduced into the wells in triplicate to ensure reproducibility of results. A control well containing only seawater and nauplii was also maintained. The microtiter plate was kept in dark conditions at room temperature for 24 hours. After the incubation period, the number of surviving nauplii was counted using an optical microscope. The percentage mortality was calculated using the following equation:

$$\text{Mortality (\%)} = \frac{A-B-N}{G-N} \times 100 \qquad (11)$$

Where
A = Number of dead nauplii after 24 h
B = Average number of dead nauplii in control samples
N = Number of dead nauplii before the experiment
G = Total number of nauplii used for the test.

4. RESULT AND DISCUSSION

4.1. Effect of Different Parameters

4.1.1 Effect of Microwave Power

Microwave power significantly influences extraction efficiency by enhancing heat generation and cell disruption. As shown in **Fig. 4.1**, the yield increased from 40% at 450 W to 62% at 540 W due to improved energy absorption and mass transfer. However, increasing power to 630 W reduced the yield to 49.5%, likely due to thermal degradation and solvent loss [**19**]. The trend indicates that moderate power enhances extraction, while excessive power reduces efficiency. Thus, 540 W was identified as the optimum condition.

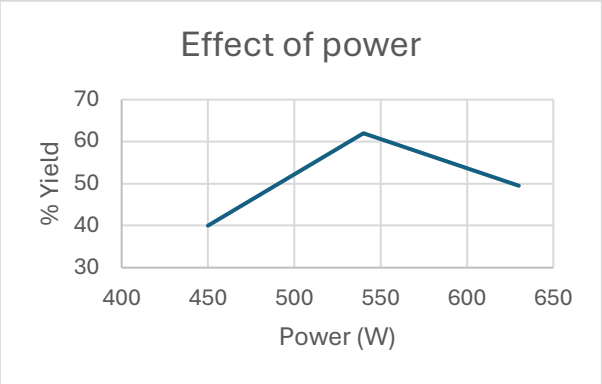

Fig. 4.1. Effect of Power

4.1.2. Effect of Time

Extraction time significantly affects yield. As shown in **Fig. 4.2**, the yield increased from 52.5% at 150 s to 65% at 180 s due to improved mass transfer and cell disruption [**20**]. However, it decreased to 48% at 210 s, likely due to thermal degradation at prolonged exposure (Sun et al., 2015). Thus, 180 s was identified as the optimum extraction time.

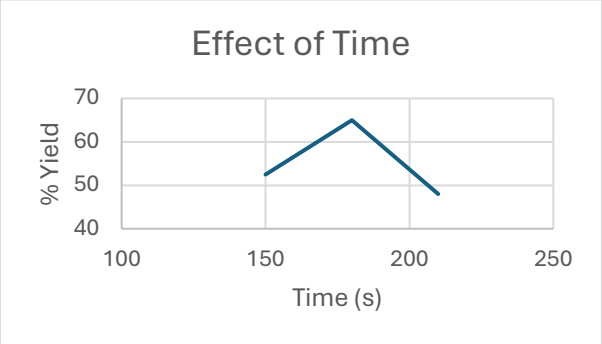

Fig. 4.2. Effect of Time

4.1.3. Effect of Concentration

Acid concentration significantly affects extraction efficiency. As shown in **Fig. 4.3**, the yield increased from 59% at 1% to a maximum of 72% at 2% due to improved solvent penetration and solubilization of compounds [**21**]. However, a slight decrease to 69% at 3% was observed, likely due to increased viscosity and reduced mass transfer. Thus, 2% was identified as the optimum concentration.

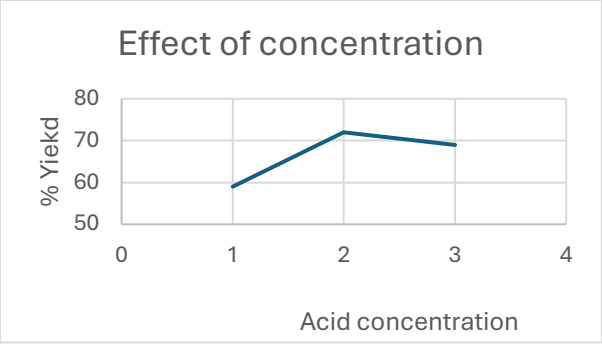

Fig. 4.3. Effect of Concentration

4.2. Response Surface Methodology (RSM)

RSM was applied to optimize microwave power, extraction time, and acid concentration using a Box–Behnken Design. The model was significant ($p < 0.001$) with $R^2 = 0.992$,

indicating good reliability. The results showed that moderate conditions improved yield, while higher levels reduced efficiency due to thermal degradation and mass transfer limitations [**22**]. The optimized conditions were 547.95 W, 161.18 s, and 2.11%, yielding 85.81%.

4.3. Cellulose yield

Microwave-assisted extraction at 540 W for 180 s yielded 70–80% cellulose, higher than conventional acid-bleaching methods (61.9%) [**23,24**]. The product appeared whiter and more fibrous, indicating effective delignification. The method is faster and more energy-efficient, highlighting its potential for sustainable cellulose extraction, though large-scale application may require suitable equipment and post-treatment.

4.4. Physicochemical Characterization

4.4.1. pH

The extracted cellulose exhibited a pH of 6.85, indicating near-neutrality and effective removal of residual acid. This is favourable for hydrogel synthesis, as acidic residues may affect polymer stability and crosslinking [**25**].

4.4.2. Solubility

The cellulose showed low solubility (0.79%) in 1% acetic acid, indicating strong intra- and intermolecular hydrogen bonding [**26**]. This behaviour is consistent with microwave-extracted cellulose, suggesting improved structural stability without compromising purity.

4.4.3. Bulk and Tapped Density

The bulk and tapped densities were 8.8 g/mL and 6.0 g/mL, respectively, indicating dense packing and low compressibility. The Hausner ratio (0.68) and Carr's Index (31.8%) suggest moderate cohesiveness and good flowability, supporting uniform dispersion and effective hydrogel formation [**27**].

4.4.4. Whiteness Index

The cellulose showed a high whiteness index (L* = 100), indicating effective removal of lignin and high purity. The smooth and uniform structure suggests minimal defects and good suitability for hydrogel formation. **Fig. 4.4** confirms improved surface quality and stability.

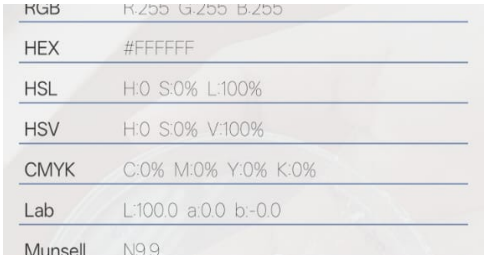

Fig. 4.4. Whiteness Index of CIELAB Value

4.5. Hydrogel Preparation and Drug Loading

A transparent cellulose–PVA network was prepared using glutaraldehyde with an H_2SO_4 catalyst, forming a stable crosslinked structure. The material showed good transparency, smooth texture, and uniformity, indicating effective crosslinking and polymer compatibility [**28, 29**]. Diclofenac sodium was successfully incorporated via the swelling–diffusion method, showing uniform distribution without surface deposition [**30**]. The structure remained intact after loading, indicating stable drug entrapment and strong polymer–drug interactions. The drug-loaded sample **Fig. 4.5** confirms its suitability for controlled drug delivery applications.

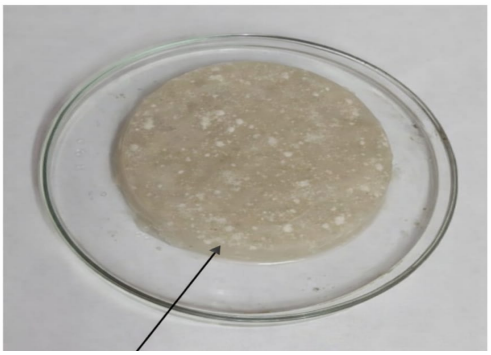

Fig. 4.5. Diclofenac sodium–loaded cellulose–PVA hydrogel

4.6. Swelling Kinetics

The swelling behaviour showed clear pH dependence, increasing with time until equilibrium. Swelling was lowest at pH 1.2, moderate at pH 5.5, and highest at pH 7.4 due to increased ionization and network expansion [**31**]. Shows limited swelling at pH 1.2 (36.5%) and higher swelling at increased pH due to electrostatic repulsion [**32**]. **Fig. 4.6** confirms maximum swelling at pH 7.4 (~196%), indicating pH-responsive behaviour suitable for controlled drug delivery [**33**].

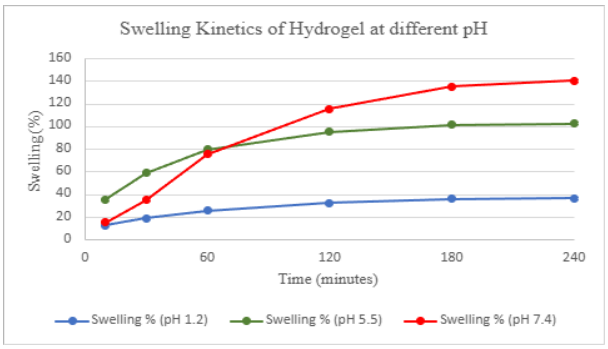

Fig. 4.6. Swelling Kinetics of Hydrogel at different pH

4.7. Porosity

The prepared hydrogel exhibited porosity in the range of 63–71%, indicating a well-developed interconnected pore structure [**34**]. This porous network facilitates solvent penetration, enhancing swelling behaviour and drug diffusion. The average porosity (~67%) supports efficient fluid uptake and sustained drug release while maintaining structural integrity [**35**].

4.8. Elasticity

The hydrogel exhibited good elastic behaviour with an elastic modulus ranging from 1850 to 2150 MPa, indicating

adequate mechanical strength and flexibility [**36, 37**]. This elasticity arises from the crosslinked polymer network, allowing deformation under stress and recovery upon release. Such balanced mechanical properties are essential for maintaining structural integrity during swelling and drug release, supporting its suitability for biomedical applications.

4.9. Hydrophilicity

The contact angle of the hydrogel ranged from 52° to 64°, indicating good hydrophilic properties. The lower contact angle reflects strong affinity towards water, promoting effective swelling and drug diffusion. This hydrophilic nature supports its suitability for biomedical and controlled drug delivery applications [**38**].

4.10. SEM Analysis

SEM micrographs revealed a rough and porous surface morphology with an interconnected three-dimensional network, indicating effective crosslinking within the polymer matrix [**39**]. This porous structure facilitates water penetration, swelling, and diffusion of diclofenac sodium, which are essential for controlled drug release. As shown in **Fig. 4.7**, the hydrogel exhibited well-defined pores of varying sizes and a rough surface with embedded drug particles, confirming successful drug incorporation. The interconnected porous network enhances water absorption and supports sustained drug release, making it suitable for biomedical and wound healing applications.

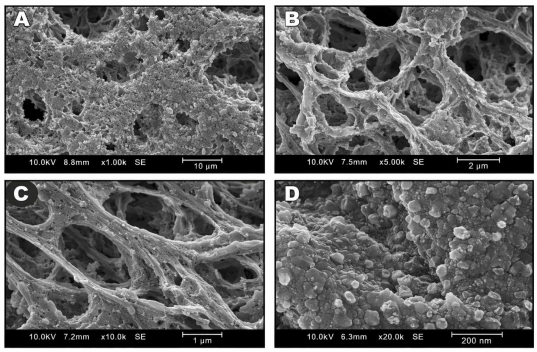

Fig. 4.7. SEM Image of Diclofenac Sodium Loaded Hydrogel

4.11. FTIR Analysis

FTIR spectra showed a broad O–H peak at 3300–3400 cm^{-1}, confirming hydroxyl groups, while the peak at ~2920 cm^{-1} corresponds to C–H stretching [**40**]. The band near 1650 cm^{-1} indicates C=O stretching, associated with diclofenac sodium, and peaks at 1100–1150 cm^{-1} confirm C–O–C linkages. As shown in **Fig. 4.8**, the drug-loaded sample retains characteristic peaks of both polymer and drug with slight shifts, indicating successful incorporation and possible hydrogen bonding without chemical degradation.

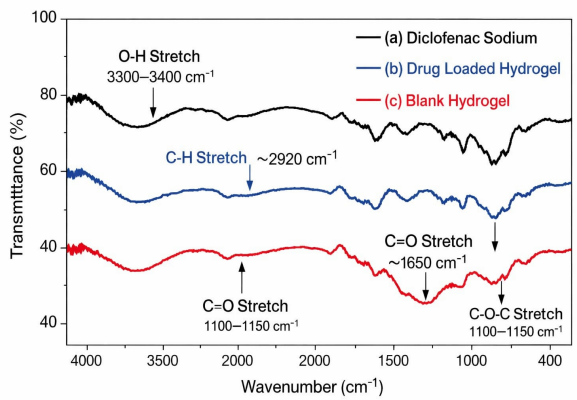

Fig.4.8. FTIR spectra of diclofenac sodium, drug-loaded hydrogel, and blank hydrogel.

4.12. Wide Angle X-ray Diffraction (WAXRD) Analysis

WAXRD analysis indicated that the hydrogel exhibits a predominantly amorphous structure, as evidenced by broad diffraction peaks and reduced crystallinity [**41**]. This suggests effective incorporation of diclofenac sodium within the polymer matrix, leading to disruption of ordered regions. **Fig. 4.9** shows a broad peak around $2\theta \approx 40–45°$, confirming uniform drug dispersion without crystalline formation. The amorphous nature enhances water absorption, swelling, and drug diffusion, thereby supporting controlled drug release and suitability for biomedical applications [**42**]

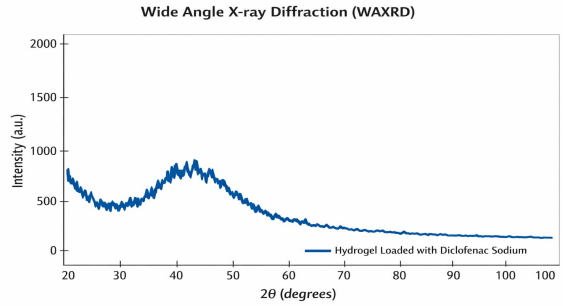

Fig. 4.9. WAXRD pattern showing the structural characteristics of the drug-loaded hydrogel.

4.13. Viscosity Study

The viscosity study revealed that the prepared hydrogel exhibits moderately high viscosity ranging from 3950 to 4320 cP, indicating the formation of a stable polymeric network. A gradual decrease in viscosity with increasing shear rate was observed, demonstrating pseudoplastic (shear-thinning) behaviour [**43, 44**]. shows this trend, where viscosity decreases from 4320 cP to 3950 cP, suggesting that the hydrogel flows easily under applied stress while maintaining structural integrity at rest. Such rheological behaviour is advantageous for drug delivery applications, as it ensures ease of application, uniform spreading, and stability of the formulation.

4.14. Drug Encapsulation Efficiency (DEE)

The drug encapsulation efficiency was evaluated to determine the drug loading capacity of the hydrogel matrix. The

prepared formulation exhibited a high encapsulation efficiency of 82.4 ± 1.2%, indicating effective incorporation and retention of diclofenac sodium within the polymer network [**45**]. This high efficiency can be attributed to strong interactions between the drug and polymer chains, along with the porous and crosslinked structure that facilitates drug entrapment. These results suggest that the hydrogel system is a promising carrier for controlled drug delivery applications [**46**].

4.15. In-vitro Drug Release Study

The in-vitro drug release study demonstrated a controlled and sustained release of diclofenac sodium from the hydrogel system. An initial faster release was observed due to surface-bound drug, followed by a slower diffusion-controlled phase through the crosslinked polymer network. The cumulative drug release reached approximately 86–89% within 180 minutes. The release data show a steady increase up to 88.4%, confirming effective drug retention and sustained release behaviour. The release profile **Fig. 4.10** exhibits a biphasic pattern, indicating initial burst release followed by controlled diffusion governed by the hydrogel structure **[47].** These results confirm the suitability of the hydrogel for controlled anti-inflammatory drug delivery.

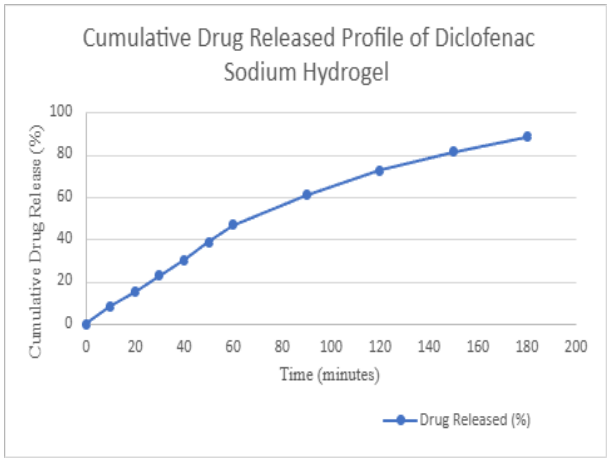

Fig. 4.10. Cumulative Drug Release (%) vs Time of Diclofenac Sodium-Loaded Cellulose-Based Hydrogel

4.16. Drug Release Kinetics

The drug release kinetics study was conducted to determine the mechanism controlling diclofenac sodium release from the hydrogel system. The release data fitted to kinetic models indicated a controlled diffusion-based pattern, with an initial moderate release followed by a sustained phase. The kinetic data show a gradual increase in drug release up to approximately 88.4% at 180 minutes, confirming sustained release behaviour. The decreasing trend in log (100–Qt) values suggests that the release rate declines as the drug concentration within the hydrogel decreases, which is consistent with diffusion-controlled release **[48].** The data showed better correlation with the first-order model, indicating concentration-dependent release governed by diffusion through the swollen polymer network. The hydrogel system demonstrates effective sustained drug delivery [**49, 50**].

4.17. Cytotoxicity study

The cytotoxicity study was conducted to evaluate the biocompatibility of the prepared hydrogel system using the brine shrimp lethality assay. The results indicated minimal toxicity, with a mortality rate of 12.6 ± 1.4%, suggesting that the hydrogel is relatively safe and biocompatible **[51].** The cytotoxicity data show that out of 30 nauplii, only 5.2 died after 24 hours, while the control group exhibited negligible mortality, confirming the reliability of the assay **[52].** The low toxicity can be attributed to the biocompatible nature of the polymeric network used in the hydrogel formulation [**53**]. Overall, these findings indicate that the developed hydrogel system is suitable for drug delivery applications without causing significant toxic effects on biological systems.

5. CONCLUSION

The present study successfully extracted cellulose from rice straw using microwave-assisted extraction and utilized it to develop a diclofenac sodium-loaded hydrogel for controlled drug delivery. Optimized conditions (540 W, 180 s, 2% acid) yielded approximately 72% cellulose. The prepared cellulose–PVA hydrogel exhibited good swelling and porosity (62–75%), supporting effective drug diffusion. Mechanical analysis showed adequate flexibility (0.42–0.71 MPa). The in-vitro drug release study indicated sustained release (~88.4% in 180 minutes) following a diffusion-controlled mechanism. Cytotoxicity results showed low mortality (12.6 ± 1.4%), confirming good biocompatibility. Overall, the hydrogel demonstrates potential for controlled anti-inflammatory drug delivery applications.

REFERENCES

1. Y. Liu, S. Li, Z. Wang, L. Wang, Ultrasound in cellulose-based hydrogel for biomedical use: from extraction to preparation, Colloids Surf. B Biointerfaces 212 (2022) 112368.
2. Y. Zhang, et al., Hydrogel-based systems for sustained drug delivery: influence of swelling behavior and crosslinking density on drug release kinetics, Int. J. Biol. Macromol. 164 (2020) 329–336.
3. D.S. Jones, G.P. Andrews, S.P. Gorman, Characterization of crosslinking effects on physicochemical and drug diffusional properties of cationic hydrogels designed as bioactive urological biomaterials, J. Pharm. Pharmacol. 57 (2005) 1251–1259.
4. X. Chen, J. Yu, Z. Zhang, C. Lu, Study on structure and thermal stability properties of cellulose fibers from rice straw, Carbohydr. Polym. 85 (2011) 245–250.
5. J.P. de Oliveira, G.P. Bruni, K.O. Lima, S.L.M. El Halal, G.S. da Rosa, A.R.G. Dias, E. da Rosa Zavareze, Cellulose fibers

extracted from rice and oat husks and their application in hydrogel, Food Chem. 221 (2017) 153–160.
6. A. Abraham, A.K. Mathew, R. Sindhu, A. Pandey, P. Binod, Potential of rice straw for bio-refining: an overview, Bioresour. Technol. 215 (2016) 29–36.
7. W. Mussoline, G. Esposito, A. Giordano, P. Lens, The anaerobic digestion of rice straw: a review, Crit. Rev. Environ. Sci. Technol. 43 (2013) 895–915.
8. N. Sharma, B.J. Allardyce, R. Rajkhowa, R. Agrawal, Rice straw-derived cellulose: a comparative study of various pre-treatment technologies and its conversion to nanofibres, Sci. Rep. 13 (2023) 16327.
9. V. Bhatt, R. Karakoti, A.K. Singh, Development and evaluation of floating biopolymeric alginate beads of diclofenac sodium obtained from Lens culinaris, World J. Pharm. Pharm. Sci. 3 (2014) 946–952.
10. S.J. Wallace, J. Li, R.L. Nation, B.J. Boyd, Drug release from nanomedicines: selection of appropriate encapsulation and release methodology, Drug Deliv. Transl. Res. 2 (2012) 284–292.
11. T.W. Ching, V. Haritos, A. Tanksale, Microwave assisted conversion of microcrystalline cellulose into value added chemicals using dilute acid catalyst, Carbohydr. Polym. 157 (2017) 1794–1800.
12. G. Gong, D. Liu, Y. Huang, Microwave-assisted organic acid pretreatment for enzymatic hydrolysis of rice straw, Biosyst. Eng. 107 (2010) 67–73.
13. M. Qian, H. Lei, E. Villota, Y. Zhao, C. Wang, E. Huo, X. Lin, High yield production of nanocrystalline cellulose by microwave-assisted dilute-acid pretreatment combined with enzymatic hydrolysis, Chem. Eng. Process. 160 (2021) 108292.
14. U. Jomnonkhaow, T. Imai, A. Reungsang, Microwave-assisted acid and alkali pretreatment of Napier grass for enhanced biohydrogen production and integrated biorefinery potential, Chem. Eng. J. Adv. 20 (2024) 100672.
15. P.A. Freitas, L.G. Santana, C. González-Martínez, A. Chiralt, Combining subcritical water extraction and bleaching with hydrogen peroxide to obtain cellulose fibres from rice straw, Carbohydr. Polym. Technol. Appl. 7 (2024) 100491
16. H.V. Chavda, C. Patel, Effect of crosslinker concentration on characteristics of superporous hydrogel, Int. J. Pharm. Investig. 1 (2011) 17–21.
17. L. Martin, C.G. Wilson, F. Koosha, L. Tetley, A.I. Gray, S. Senel, I.F. Uchegbu, The release of model macromolecules may be controlled by the hydrophobicity of palmitoyl glycol chitosan hydrogels, J. Control. Release 80 (2002) 87–100.
18. A.A. Musa, Cytotoxicity activity and phytochemical screening of Cochlospermum tinctorium rhizome, J. Appl. Pharm. Sci. 2 (2012) 155–159.
19. Y. H. Feng, T.Y. Cheng, W.G. Yang, P.T. Ma, H.Z. He, X.C. Yin, X.X. Yu, Characteristics and environmentally friendly extraction of cellulose nanofibrils from sugarcane bagasse, Ind. Crops Prod. 111 (2018) 285–291.
20. B. Sun, L. Duan, G. Peng, X. Li, A. Xu, Efficient production of glucose by microwave-assisted acid hydrolysis of cellulose hydrogel, Bioresour. Technol. 192 (2015) 253–256.
21. W. Lv, Z. Xia, Y. Song, P. Wang, S. Liu, Y. Zhang, W. Jiang, Using microwave assisted organic acid treatment to separate cellulose fiber and lignin from kenaf bast, Ind. Crops Prod. 171 (2021) 113934.
22. M. Peanparkdee, S. Iwamoto, Bioactive compounds from by-products of rice cultivation and rice processing: extraction and application, Trends Food Sci. Technol. 86 (2019) 109–117.
23. N. Kambli, S. Basak, K.K. Samanta, R.R. Deshmukh, Extraction of natural cellulosic fibers from cornhusk and its physico-chemical properties, Fibers Polym. 17 (2016) 687–694.
24. D. Trache, A. Donnot, K. Khimeche, R. Benelmir, N. Brosse, Physico-chemical properties and thermal stability of microcrystalline cellulose isolated from Alfa fibres, Carbohydr. Polym. 104 (2014) 223–230.
25. Q. An, J. Ren, X. Jia, N. Zhang, G. Fan, S. Pan, S. Cao, Valorization of citrus pomace for cellulose extraction and double-crosslinked cellulose hydrogel fabrication, Food Hydrocoll. 167 (2025) 111442.
26. H. Lu, Y. Gui, L. Zheng, X. Liu, Morphological, crystalline, thermal and physicochemical properties of cellulose nanocrystals obtained from sweet potato residue, Food Res. Int. 50 (2013) 121–128.
27. S. Cui, S. Zhang, S. Ge, L. Xiong, Q. Sun, Green preparation and characterization of size-controlled nanocrystalline cellulose via ultrasonic-assisted enzymatic hydrolysis, Ind. Crops Prod. 83 (2016) 346–352.
28. S. Bashir, Y.Y. Teo, S. Naeem, S. Ramesh, K. Ramesh, pH responsive N-succinyl chitosan/poly(acrylamide-co-acrylic acid) hydrogels and in vitro release of 5-fluorouracil, PLoS One 12 (2017) e0179250.
29. S. Hafeez, A. Islam, N. Gull, A. Ali, S.M. Khan, S. Zia, K. Anwar, S.U. Khan, T. Jamil, γ-Irradiated chitosan based injectable hydrogels for controlled release of drug (Montelukast sodium), Int. J. Biol. Macromol. 114 (2018) 890–897.
30. S.G. Nanaki, I.A. Koutsidis, I. Koutri, E. Karavas, D. Bikiaris, Miscibility study of chitosan/2-hydroxyethyl starch blends and evaluation of their effectiveness as drug sustained release hydrogels, Carbohydr. Polym. 87 (2012) 1286–1294.
31. X. Fan, et al., Polyacrylamide–gelatin–alginate hydrogels as porous wound dressing materials for enhanced tissue regeneration, Int. J. Biol. Macromol. 254 (2024) 127654.
32. M. Almasi, E. Benova, V. Zelenak, B. Madaj, V. Huntosova, J. Brus, V. Hornebecq, Cytotoxicity study and influence of SBA-15 surface polarity and pH on adsorption and release

properties of anticancer agent pemetrexed, Mater. Sci. Eng. C 109 (2020) 110552.
33. J.S. Seong, M.E. Yun, S.N. Park, Surfactant-stable and pH-sensitive liposomes coated with N-succinyl-chitosan and chitooligosaccharide for delivery of quercetin, Carbohydr. Polym. 181 (2018) 659–667.
34. F. Lv, C. Wang, P. Zhu, C. Zhang, Characterization of chitosan microparticles reinforced cellulose biocomposite sponges regenerated from ionic liquid, Cellulose 21 (2014) 4405–4418.
35. H. Pan, D. Fan, Z. Duan, C. Zhu, R. Fu, X. Li, Non-stick hemostasis hydrogels as dressings with bacterial barrier activity for cutaneous wound healing, Mater. Sci. Eng. C 105 (2019) 110118.
36. G. Kaletunc, M.D. Normand, A. Nussinovitch, M. Peleg, Determination of elasticity of gels by successive compression-decompression cycles, Food Hydrocoll. 5 (1991) 237–247.
37. M.L. Oyen, Mechanical characterisation of hydrogel materials, Int. Mater. Rev. 59 (2013) 44–59.
38. S. Kumar, J. Koh, Physicochemical, optical and biological activity of chitosan-chromone derivative for biomedical applications, Int. J. Mol. Sci. 13 (2012) 6102–6116.
39. R. Sun, S. Hughes, Fractional extraction and physicochemical characterization of hemicelluloses and cellulose from sugar beet pulp, Carbohydr. Polym. 36 (1998) 293–299.
40. H.L. Tan, L.S. Tan, Y.Y. Wong, S. Muniyandy, K. Hashim, J. Pushpamalar, Dual crosslinked carboxymethyl sago pulp/pectin hydrogel beads as potential carrier for colon-targeted drug delivery, J. Appl. Polym. Sci. 133 (2016).
41. B.K. Thakur, A. Kumar, D. Kumar, Green synthesis of titanium dioxide nanoparticles using Azadirachta indica leaf extract and evaluation of antibacterial activity, S. Afr. J. Bot. 124 (2019) 223–227.
42. Z. Wang, Y. Wang, X. Peng, Y. He, L. Wei, W. Su, J. Wu, L. Cui, Z. Liu, X. Guo, Photocatalytic antibacterial agent incorporated double-network hydrogel for wound healing, Colloids Surf. B Biointerfaces 180 (2019) 237–244.
43. Y. Pore, V. Mangrule, M. Mane, A. Chopade, Preparation, characterization and physicochemical studies of diclofenac ionic liquids, Asian J. Pharm. Pharmacol. 3 (2017) 208–214.
44. M. Maswal, O.A. Chat, A.A. Dar, Rheological characterization of multi-component hydrogel based on carboxymethyl cellulose: insight into its encapsulation capacity and release kinetics towards ibuprofen, Colloid Polym. Sci. 293 (2015) 1723–1735.
45. M. Voronova, N. Rubleva, N. Kochkina, A. Afineevskii, A. Zakharov, O. Surov, Preparation and characterization of polyvinylpyrrolidone/cellulose nanocrystals composites, Nanomaterials 8 (2018) 1–21.
46. M. Safari, M. Ghiaci, M. Jafari-Asl, A.A. Ensaf, Nanohybrid organic–inorganic chitosan/dopamine/TiO_2 composites with controlled drug-delivery properties, Appl. Surf. Sci. 342 (2015) 26–33.
47. M. Risbud, A. Hardikar, R. Bhonde, Growth modulation of fibroblasts by chitosan-polyvinyl pyrrolidone hydrogel: implications for wound management, J. Biosci. 25 (2000) 25–30.
48. P.S. Samyuktha, M.G. Dharaj, S. Rajeshkumar, In vitro study of antidiabetic effect of green synthesised titanium dioxide nanoparticles, Nat. Volatile Essent. Oils 8 (2021) 7260–7270.
49. M.F. Akhtar, N.M. Ranjha, M. Hanif, Effect of ethylene glycol dimethacrylate on swelling and metformin hydrochloride release behavior of chemically crosslinked pH-sensitive acrylic acid–polyvinyl alcohol hydrogel, DARU J. Pharm. Sci. 23 (2015).
50. M.J.A. Oliveira, E.O. Silva, L.M.A. Braz, R. Maia, V.S. Amato, A.B. Lugão, D.F. Parra, Influence of chitosan/clay in drug delivery of glucantime from PVP membranes, Radiat. Phys. Chem. 94 (2014) 194–198.
51. A. Nesic, J. Ruzic, M. Gordic, S. Ostojic, D. Micic, A. Onjia, Pectin-polyvinylpyrrolidone films: a sustainable approach to the development of biobased packaging materials, Compos. B Eng. 110 (2017) 56–61.
52. D. Solairaj, P. Rameshthangam, P. Muthukumaran, J. Wilson, Studies on electrochemical glucose sensing, antimicrobial activity and cytotoxicity of copper nanoparticle immobilized chitin nanostructure, Int. J. Biol. Macromol. 101 (2017) 668–679.
53. T. Sultana, M.M. Rana, N. Akhtar, Z. Hasan, A.H. Talukder, S.M. Asaduzzaman, Preparation and physicochemical characterization of nano-hydroxyapatite based 3D porous scaffold for biomedical application, Adv. Tissue Eng. Regen. Med. 3 (2017).